Published for SISSA by Springer

Received: June 10, 2024
Revised: July 18, 2024
Accepted: July 22, 2024
Published: August 13, 2024

Three-loop corrections to Higgs boson pair production: reducible contribution

Joshua Davies,[a] **Kay Schönwald**,[b] **Matthias Steinhauser**[c] and **Marco Vitti**[c,d]

[a]*Department of Mathematical Sciences, University of Liverpool, Liverpool L69 3BX, U.K.*
[b]*Physik-Institut, Universität Zürich, Winterthurerstrasse 190, Zürich 8057, Switzerland*
[c]*Institut für Theoretische Teilchenphysik, Karlsruhe Institute of Technology (KIT), Wolfgang-Gaede Straße 1, Karlsruhe 76128, Germany*
[d]*Institut für Astroteilchenphysik, Karlsruhe Institute of Technology (KIT), Hermann-von-Helmholtz-Platz 1, Eggenstein-Leopoldshafen 76344, Germany*

E-mail: j.o.davies@liverpool.ac.uk, kay.schoenwald@physik.uzh.ch, matthias.steinhauser@kit.edu, marco.vitti@kit.edu

Abstract: We compute three-loop corrections to the process $gg \to HH$ originating from one-particle reducible diagrams. This requires the computation of two-loop corrections to the gluon-gluon-Higgs vertex with an off-shell gluon. We describe in detail our approach to obtain semi-analytic results for the vertex form factors and present results for the two form factors contributing to Higgs boson pair production.

Keywords: Higgs Production, Higgs Properties, Higher-Order Perturbative Calculations

ArXiv ePrint: 2405.20372

https://doi.org/10.1007/JHEP08(2024)096

JHEP08(2024)096

Contents

1 Introduction and notation

The simultaneous production of two Higgs bosons is the most promising process from which we can obtain information about the Higgs boson's self coupling. At hadron colliders it is dominated by the gluon fusion production channel, which at leading order (LO) receives contributions from "triangle"- and "box"-type diagrams. The LO form factors and cross section were computed more than 35 years ago [1, 2]. Next-to-leading order (NLO) corrections with full dependence on the top quark mass are available in numerical form from refs. [3–5]. "Semi-analytic expressions" which are essentially equivalent to the numerical results, but more flexible in that mass values can be adjusted, have been computed in refs. [6, 7]. Furthermore there are a number of approximations which are valid in certain regions of phase space (see, e.g., refs. [8–15]).

In refs. [16, 17] it has been pointed out that the renormalization scheme dependence of the top quark mass induces a sizeable uncertainty on the NLO Higgs boson pair cross section. This motivates a next-to-next-to-leading order (NNLO) calculation of the Higgs boson pair production cross section. The most challenging part in this context is the three-loop virtual correction to $gg \to HH$. This can be divided into two classes: (i) diagrams where both Higgs bosons couple to the same top quark loop (as shown in figure 1(a)), and (ii) diagrams where the Higgs bosons couple to different top quark loops. For the latter class there are one-particle irreducible and one-particle reducible contributions (as shown in figures 1(b) and 1(c) respectively). The irreducible and reducible contributions are, separately, neither finite nor gauge-parameter independent, which has already been discussed in refs. [18, 19].

The large top quark mass limit of the complete set of diagrams has been considered in refs. [18, 20], where five expansion terms in $1/m_t^2$ were computed. The light-fermion contribution to class (i) has been computed in ref. [21] for $t = 0$ and $m_H = 0$, which is a promising method to obtain an approximation of the unknown exact result.

JHEP08(2024)096

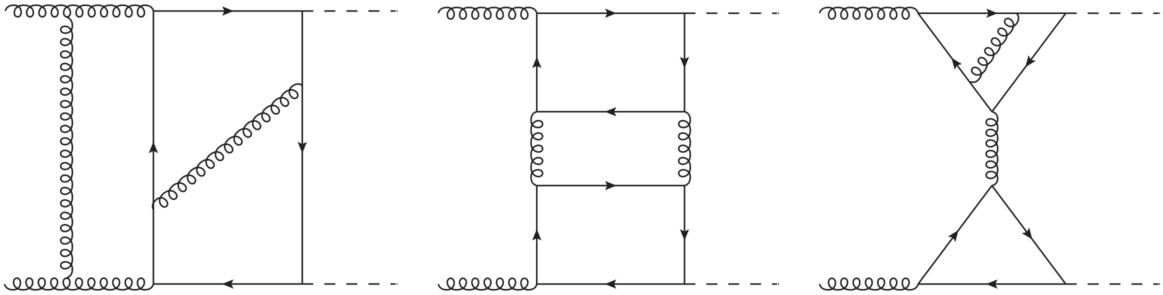

(a) (b) (c)

Figure 1. Classification of the three-loop virtual corrections to $gg \to HH$. (a) shows "class (i)", where both Higgs bosons couple to the same top quark loop. (b) and (c) show "class (ii)", where each Higgs boson couples to a different top quark loop, in a one-particle irreducible and reducible way, respectively.

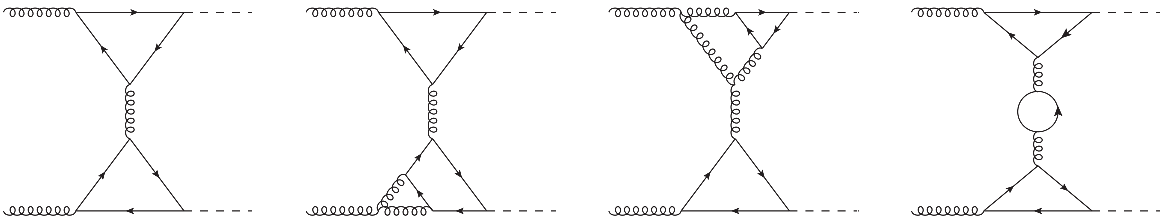

Figure 2. Sample two- and three-loop Feynman diagrams contributing to the one-particle reducible part of $gg \to HH$. Solid, dashed and curly lines represent top quarks, Higgs bosons and gluons, respectively.

We point out that the diagrams of class (ii) cannot be evaluated using the same approach as in ref. [21], which is based on a Taylor expansion of the amplitude. Rather, an asymptotic expansion is necessary, because of the presence of t-channel cuts through massless lines. This is also true for the reducible contribution which we consider in this paper. It can be composed from one- and two-loop corrections to the gluon-gluon-Higgs vertex with an off-shell gluon and one-loop corrections to the gluon propagator. Some sample Feynman diagrams are depicted in figure 2.

For completeness we briefly repeat the definition of the form factors for $g(q_1)g(q_2) \to H(q_3)H(q_4)$, with all momenta q_i defined to be incoming (thus, $q_4 = -q_1 - q_2 - q_3$). The amplitude can be decomposed into two Lorentz structures

$$\mathcal{M}^{ab} = \varepsilon_{1,\mu}\varepsilon_{2,\nu}\mathcal{M}^{\mu\nu,ab} = \varepsilon_{1,\mu}\varepsilon_{2,\nu}\delta^{ab}X_0 s \left(F_1 A_1^{\mu\nu} + F_2 A_2^{\mu\nu}\right) , \tag{1.1}$$

where a and b are adjoint colour indices and $s = (q_1 + q_2)^2$ is the squared partonic centre-of-mass energy. The two Lorentz structures are given by

$$\begin{aligned} A_1^{\mu\nu} &= g^{\mu\nu} - \frac{1}{q_{12}} q_1^\nu q_2^\mu , \\ A_2^{\mu\nu} &= g^{\mu\nu} + \frac{1}{p_T^2 q_{12}} \left(q_{33} q_1^\nu q_2^\mu - 2q_{23} q_1^\nu q_3^\mu - 2q_{13} q_3^\nu q_2^\mu + 2q_{12} q_3^\mu q_3^\nu\right) , \end{aligned} \tag{1.2}$$

with

$$q_{ij} = q_i \cdot q_j\,, \qquad p_T^2 \;=\; \frac{2q_{13}q_{23}}{q_{12}} - q_{33} \;=\; \frac{tu - m_H^4}{s} \tag{1.3}$$

where s, $t = (q_1 + q_3)^2$ and $u = (q_2 + q_3)^2$ are Mandelstam variables which fulfill $s + t + u = 2m_H^2$. The quantity X_0 is given by

$$X_0 = \frac{G_F}{\sqrt{2}} \frac{\alpha_s(\mu)}{2\pi} T_F\,, \tag{1.4}$$

with $T_F = 1/2$, G_F is Fermi's constant and $\alpha_s(\mu)$ is the strong coupling constant evaluated at the renormalization scale μ.

We define the expansion in α_s of the form factors as

$$F = F^{(0)} + \frac{\alpha_s(\mu)}{\pi} F^{(1)} + \left(\frac{\alpha_s(\mu)}{\pi}\right)^2 F^{(2)} + \cdots\,. \tag{1.5}$$

The one-particle reducible contributions which we focus on here contribute for the first time at two loops, to $F^{(1)}$. We denote their contribution to F_1 and F_2 by $F^{(1)}_{\rm dt1}$ and $F^{(1)}_{\rm dt2}$, respectively. At this order they have been computed in ref. [9], where they are given as exact expressions in all parameters. In this paper we reproduce these results in an expansion for $m_H \to 0$ and add the terms of order ϵ and ϵ^2 at two loops, which are necessary for renormalization and infrared subtraction at three loops, and we compute the corresponding contributions at three-loop order, $F^{(2)}_{\rm dt1}$ and $F^{(2)}_{\rm dt2}$. We point out that in our calculation we are not including the reducible contribution from diagrams with an off-shell Higgs propagator, since we assign those diagrams to class (i).

The main ingredient for our calculation are two-loop corrections to the $gg \to H$ vertex with an off-shell gluon, as can be seen from figure 2. We denote this as $gg^* \to H$. We are not aware of public results for this amplitude, which might be an ingredient also for other calculations. In the next section we describe our approach to compute this building block in detail. In section 3 we then present our results for the form factors $F_{\rm dt1}$ and $F_{\rm dt2}$ before we conclude in section 4.

2 Calculation of the $gg^* \to H$ vertex at two loops

2.1 $gg^* \to H$ form factors

In this section we describe the calculation of the $gg^* \to H$ building block, which we have to consider up to two-loop order. We introduce the three-point amplitude $\mathcal{V}^{\alpha\beta}(q_s, q_2)$ for the interaction of an off-shell gluon, an on-shell gluon and a Higgs boson. Assuming that the off-shell gluon has momentum q_s, the on-shell gluon q_2 and that all momenta are incoming we have $(q_s + q_2)^2 = m_H^2$ and the most general Lorentz decomposition of the amplitude is

$$\mathcal{V}^{\alpha\beta}(q_s, q_2) = V_0 \left(F_a\, g^{\alpha\beta}(q_s \cdot q_2) + F_b\, q_s^\alpha q_2^\beta + F_c\, q_2^\alpha q_s^\beta + F_d\, q_s^\alpha q_s^\beta + F_e\, q_2^\alpha q_2^\beta\right)\,, \tag{2.1}$$

where the form factors F_x are dimensionless. For the expansion in α_s we follow eq. (1.5). The normalization factor V_0 is chosen such that

$$F_a^{(0)}(s = 0, m_H = 0) = \frac{4}{3}\,. \tag{2.2}$$

JHEP08(2024)096

Furthermore, we decompose $F_x^{(1)}$ according to the SU(N_c) colour factors $C_A = N_c$ and $C_F = (N_c^2 - 1)/(2N_c)$

$$F_x^{(1)} = C_A F_x^{(1),C_A} + C_F F_x^{(1),C_F} \,. \tag{2.3}$$

Note that $F_a, \ldots, F_e$ are not all independent. Typically, imposing the Ward identities allows one to derive relations among them. However, since one gluon is off-shell, more structures give a non-zero contribution compared to the case in which both gluons are on-shell. The Ward identities in our case are obtained by the simultaneous contraction of both gluon momenta with the amplitude,

$$q_{s,\alpha} q_{2,\beta} \mathcal{V}^{\alpha\beta}(q_s, q_2) = 0, \tag{2.4}$$

which leads to the following relation between the form factors

$$F_d = -\frac{(F_a + F_c)(m_H^2 - q_s^2)}{2q_s^2} \,. \tag{2.5}$$

For the calculation of the form factors for Higgs pair production F_b and F_e are not needed. We note that at one-loop order we find $F_d^{(0)} = 0$, so that the above relation implies that $F_c^{(0)} = -F_a^{(0)}$, as in the case of two on-shell gluons. At two-loop order, however, $F_d^{(1)}$ is not zero; we have verified that our results satisfy eq. (2.5). At two-loop order $F_d^{(1)}$ only has a contribution proportional to the colour factor C_A.

The one-loop form factor $F_a^{(0)}$ is finite and gauge-parameter independent. At two-loop order the form factors depend on the QCD gauge parameter ξ and furthermore develop $1/\epsilon$ poles, which have both ultraviolet and infrared origin. The ξ dependence and $1/\epsilon$ poles are also present in the three-loop one-particle reducible parts of the Higgs boson pair production form factors F_{dt1} and F_{dt2}. Here the ξ dependence cancels after the combination with the contribution (b) from figure 1, as we have shown previously in ref. [18] in the context of the large top quark mass expansion. The cancellation of the ultraviolet $1/\epsilon$ poles requires additionally the renormalization of the top quark mass, the strong coupling constant and the gluon wave function. The infrared poles must be subtracted using an appropriate prescription (see, e.g., ref. [22]), or the real-radiation contributions must be added. In this paper we present bare results, both for the $gg^* \to H$ vertex and the $gg \to HH$ form factors F_{dt1} and F_{dt2}, with explicit dependence on ξ and ϵ.

2.2 Workflow

In the following we describe the workflow for the computation of the $gg^* \to H$ vertex. As described above, we give the off-shell gluon the momentum q_s. When we use the resulting building block to construct F_{dt1} and F_{dt2} for $gg \to HH$, we will have either $q_s^2 = t$ or $q_s^2 = u$. Thus, the relevant kinematic region for the $gg^* \to H$ vertex has $q_s^2 < 0$.

We first generate the amplitude in terms of Lorentz-scalar functions using our usual chain of programs (`qgraf` [23], `tapir` [24], `exp` [25, 26] and the in-house `FORM` [27] code "`calc`"). We then perform the integration-by-parts reduction to master integrals using `Kira` [28], arriving at 4 and 46 master integrals at one and two loops, respectively. Up to this point, we retain exact dependence on the kinematic parameters q_s^2, m_H and m_t.

JHEP08(2024)096

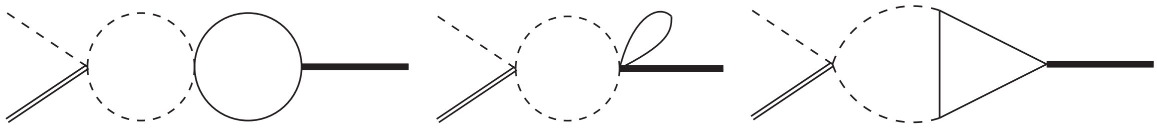

Figure 3. The three out of the 46 two-loop master integrals which have a soft and hard contribution. Dashed lines denote massless internal and external legs, while solid thin lines are used for massive internal legs with mass m_t. Double lines and solid thick lines denote massive external legs with virtuality q_s^2 and mass m_H, respectively.

The next step is to compute the master integrals. Here we distinguish two kinematic regions, which allows us to obtain compact (semi-)analytic results for the form factors. In the first region, we expand the master integrals around $m_H \to 0$, which leads to a good approximation for larger values of $|q_s^2|$. For smaller values we instead expand for $|q_s^2| \to 0$. In the following two subsections, we describe our approach for each region.

2.3 Small m_H expansion

At one-loop order the expansion of the master integrals for small m_H is a Taylor expansion, which is conveniently realized with the help of `LiteRed` [29]. At two-loop order one must consider an asymptotic expansion based on two regions; in the hard region we can again use `LiteRed` for a Taylor expansion in m_H. The second region arises from diagrams which have an external momentum $(q_s + q_2)^2 = m_H^2$ and at the same time a cut through gluon lines. Among the 46 two-loop master integrals there are three such integrals, which are shown in figure 3. None of them depend on q_s^2, thus the expansion for $m_H \to 0$ is equivalent to the large-m_t expansion which is straightforward to perform using `exp`. We want to stress again that although after expanding in the external Higgs mass the kinematics are similar to the on-shell $gg \to H$ form factor, the topologies we have to consider are different since the off-shell gluon can couple to massless internal lines.

After the expansion in m_H, in the hard region we obtain new integral families. For the integration-by-parts reduction we use again `Kira` and obtain 25 master integrals. Their internal lines are either massless or have mass m_t. Two of the external lines are massless and one has the off-shell squared momentum q_s^2; the master integrals depend only on the ratio q_s^2/m_t^2.

The one-loop master integrals can be computed analytically in terms of harmonic polylogarithms [30]. At two-loop order the analytic structure of the master integrals is much more involved since one of the sectors leads to elliptic integrals as has been shown in ref. [31]. Therefore, we use for the evaluation of the master integrals at two-loop order the "expand and match" approach [32–35] which uses the differential equations for the master integrals to construct deep generalized expansions around properly chosen values of q_s^2/m_t^2, with high-precision numerical coefficients. The boundary values at $q_s^2/m_t^2 \to 0$ are obtained analytically using the large-m_t expansion, and then transported numerically to the other expansion points with high precision.

Using this approach we obtain expansions for each master integral up to order m_H^8, where the coefficients are "semi-analytic" piecewise functions of q_s^2/m_t^2. Thus a flexible

JHEP08(2024)096

implementation in a computer code is possible, which allows for a straightforward modification of all input parameters.

2.4 Low energy expansion

In order to cover the small $|q_s^2|$ region, we instead expand the master integrals in the limit $q_s^2 \to 0$. Note that this expansion is only required at the two-loop level; at one loop, the small m_H expansion covers the full kinematic region because the external gluons couple only to massive top quarks.

The expansion for $q_s^2 \to 0$ is also an asymptotic expansion with two regions which we denote as "hard" and "soft" in the following. We construct the expansion from the differential equation by separating the two branches of the asymptotic expansion and deriving power series solutions, as is usually done in the "expand and match" approach. In the low energy expansion it is again possible to fix the boundary values analytically.

The expansion in the hard region can be realized by a Taylor series in the off-shell momentum q_s. The resulting integrals are the same as for on-shell Higgs production at two-loop order [36–40]. We have re-derived the solutions by solving the system of differential equations utilizing the algorithm of ref. [41] implemented with the help of the packages `HarmonicSums` [42–53] and `Sigma` [54, 55]. The only boundary condition necessary is the two-loop tadpole; the results can be expressed in terms of harmonic polylogarithms [30] of argument x_{m_H} defined by

$$\frac{m_H^2}{m_t^2} = -\frac{(1-x_{m_H})^2}{x_{m_H}} . \tag{2.6}$$

The boundary conditions in the soft region are obtained by direct integration and summation techniques. We first reveal the scaling of the α-parameters of the Schwinger parameterization of the Feynman integrals with the help of `asy` [56] and integrate them in terms of a one-dimensional Mellin-Barnes representation. The remaining integral is solved by summing residues symbolically with `EvaluateMultiSums` [57, 58]. The final step is to convert the infinite sums into a representation in terms of harmonic polylogarithms, using `HarmonicSums`.

Let us demonstrate the steps explicitly for a simple example. One of the master integrals which we have to calculate in the limit $q_s^2 \to 0$ is given by

$$I_{21} = \int \frac{\mathrm{d}^d k_1}{(2\pi)^d} \int \frac{\mathrm{d}^d k_2}{(2\pi)^d} \frac{1}{[m_t^2 - k_1^2][m_t^2 - (k_2 - q_s - q_2)^2][-(k_1 - k_2 + q_s)^2][-(k_1 - k_2)^2]} . \tag{2.7}$$

`asy` finds the soft region $I = \{0, 0, -1, -1\}$ and the hard region $I_h = \{0, 0, 0, 0\}$. In the soft region we obtain the one-dimensional Mellin-Barnes representation

$$I_{21}^{(I)} = \frac{1}{2\pi i} \mathcal{N} \int\limits_{-i\infty}^{+i\infty} \mathrm{d}\sigma (-\rho)^\sigma \frac{\Gamma(1-\epsilon)\Gamma(\epsilon)\Gamma(-\sigma)\Gamma^2(1+\sigma)\Gamma(1-\epsilon+\sigma)\Gamma(\epsilon+\sigma)}{\Gamma(2-2\epsilon+\sigma)\Gamma(2+2\sigma)} , \tag{2.8}$$

with $\rho = m_H^2/m_t^2$ and $\mathcal{N} = (-s/m_t^2)^{-\epsilon}\exp(-2\epsilon\gamma_E)$. By closing the integration contour to the right and using Cauchy's residue theorem we can turn the integration into an infinite sum

$$\begin{aligned} I_{21}^{(I)} &= \mathcal{N}\sum_{k=0}^{\infty}\rho^k\Gamma(1-\epsilon)\Gamma(\epsilon)\frac{\Gamma(1+k)\Gamma(1-\epsilon+k)\Gamma(\epsilon+k)}{\Gamma(2-2\epsilon+k)\Gamma(2+2k)} \\ &= \left(\frac{-s}{m_t^2}\right)^{-\epsilon}\left\{\frac{1}{\epsilon^2}+\frac{1}{\epsilon}\left[\frac{1}{16}\left(32+44\rho-12\rho^2+\rho^3\right)-\frac{(\rho(4-\rho))^{3/2}}{4\rho^2}G_1-\frac{1}{4\rho}G_1^2\right]+\mathcal{O}(\epsilon^0)\right\}, \end{aligned} \tag{2.9}$$

with

$$G_1 = \int_0^\rho \mathrm{d}t\sqrt{t}\sqrt{4-t}\,. \tag{2.10}$$

The symbolic summation has been performed with `EvaluateMultiSums` and `HarmonicSums` and for brevity we do not show higher terms in the ϵ-expansion here, though they are needed for the full calculation. Finally we can transform to the variable defined in eq. (2.6) to obtain

$$I_{21}^{(I)} = \mathcal{N}\left\{\frac{1}{\epsilon^2}+\frac{1}{\epsilon}\left[5+\frac{1+x_{m_H}}{1-x_{m_H}}H_0(x_{m_H})-\frac{x_{m_H}}{(1-x_{m_H})^2}H_0^2(x_{m_H})\right]+\mathcal{O}(\epsilon^0)\right\}. \tag{2.11}$$

The final results for the master integrals are obtained by summing the contributions of both asymptotic regions. Finally, after inserting the master integrals into the expanded amplitude, we obtain a consistent power-log expansion (we compute 19 terms) in the limit $q_s^2 \to 0$ of the form factors where the coefficients are given by analytic expressions depending on the variable x_{m_H} and only harmonic polylogarithms are necessary. Therefore, evaluating the amplitude for small values of q_s^2 is fast.

We stress here that although we have fully analytic results for the low energy expansion, the small m_H expansion of section 2.3 is "semi-analytic".

2.5 One-loop results for the $gg^* \to H$ vertex

Let us start with the discussion of the one-loop result for the $gg^* \to H$ vertex with an off-shell gluon, which we need up to order ϵ. Here the expansion in m_H works very well, even for small values of $|q_s^2|$. For convenience we present explicit results for[1] $F_a^{(0)}$ including terms up to $\mathcal{O}(m_H^2)$ and $\mathcal{O}(\epsilon)$. We set $\mu = m_t$ for brevity. Expansions up to order m_H^4 and ϵ^2 and with full dependence on the renormalization scale can be found in the supplementary material of this paper.[2] Our result reads

$$\begin{aligned} F_a^{(0)} = &\frac{24x}{(1-x)^2}+\frac{8x(1+x)H_0}{(1-x)^3}+\frac{4x\left(1-6x+x^2\right)H_{0,0}}{(1-x)^4}+\epsilon\left[\frac{56x}{(1-x)^2}+\frac{24x(1+x)H_0}{(1-x)^3}\right. \\ &+\frac{8x\left(1-2x-x^2\right)H_{0,0}}{(1-x)^4}-\frac{16x(1+x)H_{-1,0}}{(1-x)^3}+\frac{4x\left(1-6x+x^2\right)H_{0,0,0}}{(1-x)^4} \\ &-\frac{8x\left(1-6x+x^2\right)H_{0,-1,0}}{(1-x)^4}-\frac{12x\left(1-6x+x^2\right)\zeta(3)}{(1-x)^4}-\pi^2\left(\frac{4x(1+x)}{3(1-x)^3}\right. \end{aligned}$$

[1] Note that the other form factors are either zero, or are not needed for F_{dt1} and F_{dt2}.
[2] Terms beyond m_H^4 are very small for all q_s^2 values.

JHEP08(2024)096

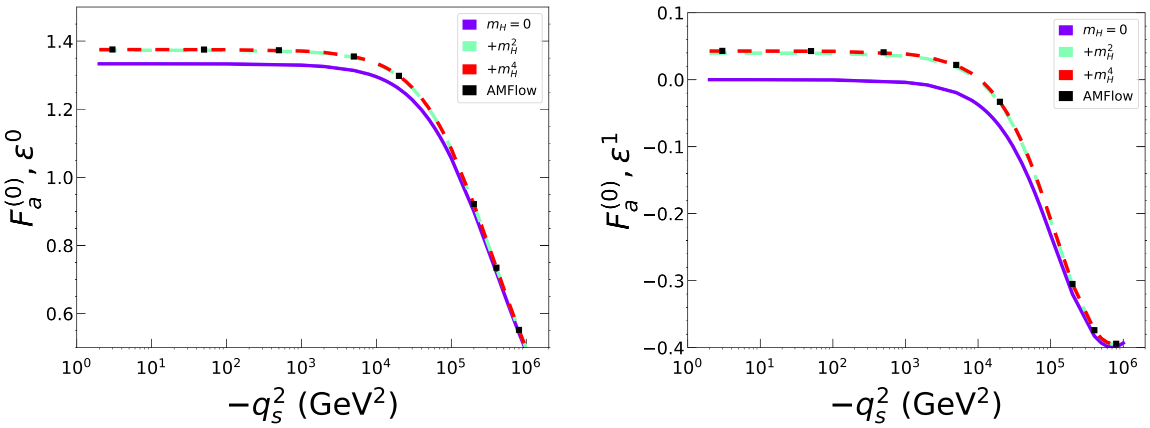

Figure 4. $F_a^{(0)}$ as a function of q_s^2. Both the ϵ^0 (left) and ϵ^1 terms (right) are shown.

$$
\begin{aligned}
&+\frac{2x\left(1-6x+x^2\right)H_0}{3(1-x)^4}\Bigg)\Bigg] + \frac{m_H^2}{m_t^2}\Bigg\{\frac{2x\left(1-74x+x^2\right)}{3(1-x)^4} - \frac{16x^2(1+x)H_0}{(1-x)^5} \\
&-\frac{4x^2\left(1-10x+x^2\right)H_{0,0}}{(1-x)^6} + \epsilon\Bigg[-\frac{112x^2}{(1-x)^4} - \frac{48x^2(1+x)H_0}{(1-x)^5} + \frac{32x^2(1+x)H_{-1,0}}{(1-x)^5} \\
&-\frac{16x^2\left(1-2x-x^2\right)H_{0,0}}{(1-x)^6} - \frac{4x^2\left(1-10x+x^2\right)H_{0,0,0}}{(1-x)^6} + \frac{8x^2\left(1-10x+x^2\right)H_{0,-1,0}}{(1-x)^6} \\
&+\pi^2\left(\frac{8x^2(1+x)}{3(1-x)^5} + \frac{2x^2\left(1-10x+x^2\right)H_0}{3(1-x)^6}\right) + \frac{12x^2\left(1-10x+x^2\right)\zeta_3}{(1-x)^6}\Bigg]\Bigg\} \\
&+\mathcal{O}(m_H^4) + \mathcal{O}(\epsilon^2)\,, \qquad (2.12)
\end{aligned}
$$

with $q_s^2/m_t^2 = -(1-x)^2/x$ and $H_{\vec{w}} \equiv H_{\vec{w}}(x)$.

In figure 4 we show $F_a^{(0)}$ as a function of q_s^2, at several expansion depths in m_H. Furthermore we show results obtained from the un-expanded amplitude, with the four master integrals evaluated numerically using `AMFlow` [59]. For the values for the top quark and Higgs boson masses we use

$$
m_t = 175\,\text{GeV} \qquad \text{and} \qquad m_H = 125\,\text{GeV}\,. \qquad (2.13)
$$

We observe a rapid convergence of the m_H expansion, and very good agreement with the numerical results. For example, for $q_s^2 = -3\,\text{GeV}^2$ the deviation of the m_H^4 expansion from the numerical results is about 0.01%, 0.7% and 0.02% for the ϵ^0, ϵ^1 and ϵ^2 terms, respectively. For all practical purposes it is sufficient to work with the small m_H approximation, including terms up to order m_H^4; these expressions are much more convenient to work with, since only simple harmonic polylogarithms are present.

2.6 Two-loop results for the $gg^* \to H$ vertex

We first want to discuss the quality of our approximations. In the case of the low energy expansion we use the master integrals from section 2.4, insert them into the amplitude and expand the whole amplitude consistently in q_s^2. This leads to compact expressions.

JHEP08(2024)096

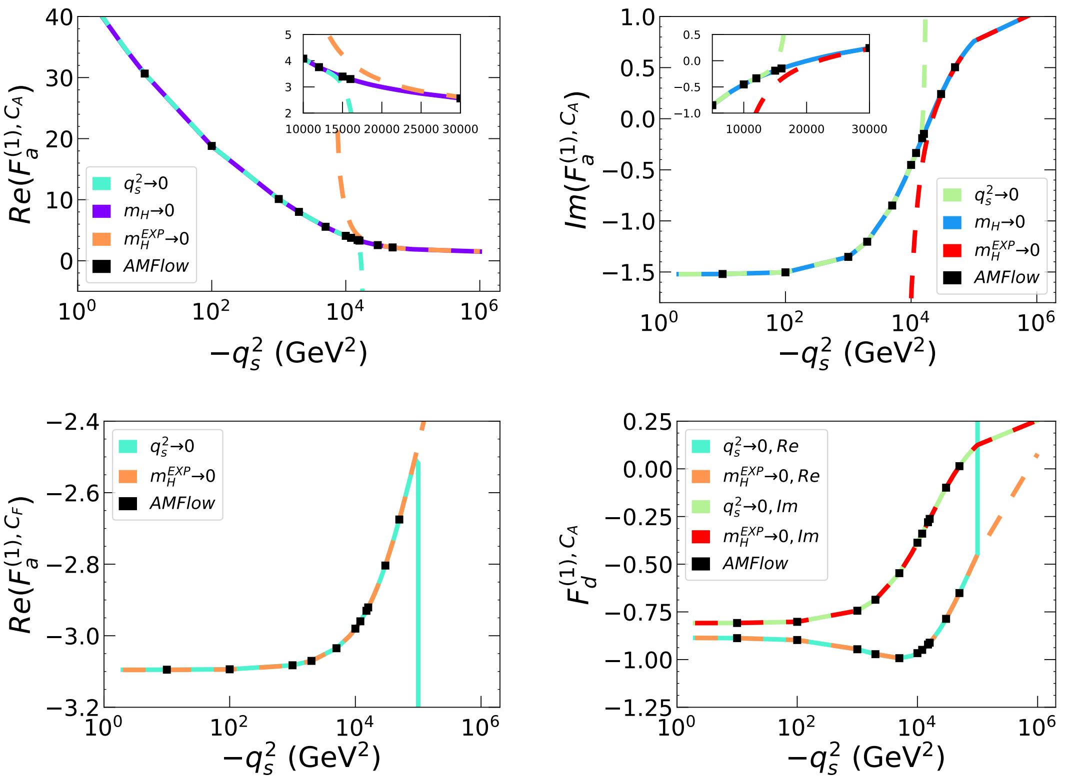

Figure 5. $F_a^{(1)}$ and $F_d^{(1)}$ as a function of q_s^2.

If $|q_s^2|$ is sufficiently large we can construct a consistent expansion in m_H, i.e., after inserting the m_H-expanded master integrals into the amplitude we expand the whole expression in m_H, up to order m_H^8. In the plots the corresponding curves have the label "$m_H^{\rm EXP} \to 0$". However, as we will see below, in the intermediate q_s^2 region, $100\,\text{GeV} \lesssim \sqrt{|q_s^2|} \lesssim 170\,\text{GeV}$, it is crucial to *not* expand the coefficients of the master integrals in m_H, in order to obtain stable numerical results for $F_a^{(1),C_A}$. In the plots the corresponding curves are denoted by "$m_H \to 0$". The form factor $F_a^{(1),C_F}$ does not have this problem, since there are no contributing Feynman diagrams with a massless cut. As a consequence, $F_a^{(1),C_F}$ can be treated in the same way as the one-loop form factor, i.e., the consistent m_H expansion covers the whole phase space. This we also observe for $F_d^{(1)}$ although it obtains contributions from diagrams with massless cuts; see discussion below.

Note that in the latter case where we use m_H-expanded master integrals but do not expand their coefficients, there is no analytic cancellation of the spurious higher-order ϵ poles, which in this case are $1/\epsilon^2$ and $1/\epsilon^3$. However, their coefficients are small, typically four to five orders of magnitude smaller than the coefficient at order ϵ^0; we take this to be a measure of our numerical accuracy.

In figure 5 we show the finite parts of the two-loop form factors $F_a^{(1)}$ and $F_d^{(1)}$ as a function of q_s^2. For the renormalization scale we have chosen $\mu^2 = m_t^2$. For convenience we choose a logarithmic scale for the q_s^2 axis which enhances the region for small values of $|q_s^2|$. The squares in figure 5 correspond to exact results where numerical values for the 46 master integrals have been obtained with `AMFlow` [59]. The excellent agreement with our results justifies our approximations in the various q_s^2 regions.

For $F_a^{(1),C_A}$ we show the approximation for small $|q_s^2|$ and the two versions of the small-m_H expansion (as described above). We observe that there is a small gap, close to $-q_s^2 \approx 10^4\,\text{GeV}^2$, between the "$q_s^2 \to 0$" and "$m_H^{\text{EXP}} \to 0$" expansions (see inset plot). It is here that the "$m_H \to 0$" expansion must be used. The latter works well for fairly small values of q_s^2. Note, however, that for $|q_s^2| < 10\,\text{GeV}^2$ the deviation between the "$q_s^2 \to 0$" and "$m_H \to 0$" result is of the order 1% or higher, thus the use of the "$q_s^2 \to 0$" expansion is preferable. For $F_a^{(1),C_F}$ and $F_d^{(1),C_A}$ we only show the "$q_s^2 \to 0$" and "$m_H \to 0$" curves and observe that the m_H-expanded approximation covers the whole q_s^2 range. For $F_a^{(1),C_F}$ the two approximations agree far below the per cent level for $|q_s^2| \lesssim 90\,000\,\text{GeV}^2$. Also for $F_d^{(1),C_A}$ one observes very good agreement of the consistent m_H expansion with the results from the q_s-expansion and the numerical results (black squares). It is interesting to note that the q_s-expansion also works well up to quite high values of $|q_s^2|$. In the case of the imaginary part it shows good agreement with the m_H expansion even for $|q_s^2| \approx 10^6\,\text{GeV}^2$. The agreement is below 0.01% for $|q_s^2| \lesssim 100\,000\,\text{GeV}^2$ both for the real and imaginary part.

Thus, our scheme for the numerical evaluation of $F_a^{(1),C_A}$ is as follows: for $|q_s^2| \lesssim 5\,000\,\text{GeV}^2$ we use the q_s^2-expansion, for $5\,000\,\text{GeV}^2 \lesssim |q_s^2| \lesssim 80\,000\,\text{GeV}^2$ we use the "$m_H \to 0$" expansion, and for $|q_s^2| \gtrsim 80\,000\,\text{GeV}^2$ we use the "$m_H^{\text{EXP}} \to 0$" expansion.

At this point a comment is in order on the relevant values for $|q_s^2|$, once the $gg^* \to H$ vertex is used to compute the $gg \to HH$ form factors F_{dt1} and F_{dt2}. In the case of double Higgs production, if we consider e.g. $q_s^2 = t$, the "$m_H^{\text{EXP}} \to 0$" expansion is sufficient in order to cover the phase-space region where $p_T \gtrsim 280\,\text{GeV}$, for every value of $\sqrt{s}$. Instead, the "$m_H \to 0$" and the "$m_H^{\text{EXP}} \to 0$" expansions are required for $p_T \gtrsim 70\,\text{GeV}$. Thus, the small-$m_H$ expansion covers the major part of the phase space. Let us finally mention that for $F_a^{(1),C_A}$ it would be possible to use the "$m_H \to 0$" even for $q_s^2 = -100\,\text{GeV}^2$. In that case the q_s expansion is only necessary for $p_T = 10\,\text{GeV}$ or smaller and $\sqrt{s}$ above $10\,000\,\text{GeV}$.

3 NNLO one-particle reducible results for $gg \to HH$

In this section we discuss results for the form factors $F_{\text{dt1}}^{(1)}$, $F_{\text{dt2}}^{(1)}$, $F_{\text{dt1}}^{(2)}$ and $F_{\text{dt2}}^{(2)}$, as introduced after eq. (1.5). Sample Feynman diagrams are shown in figure 2. They can easily be constructed from the general structure of the $gg^* \to H$ vertex from eq. (2.1), using the off-shell gluon momentum to connect the two vertices via a gluon propagator. There are diagrams with either $q_s^2 = t$ or $q_s^2 = u$. We additionally must include the one-loop correction to the gluon propagator, multiplied by a pair of one-loop $gg^* \to H$ vertices. This leads to the following compact formulae for the NNLO form factors,

$$F_{\text{dt1}}^{(2)} = \tilde{F}_{\text{dt1}}^{(2)}(t) + \tilde{F}_{\text{dt1}}^{(2)}(u), \qquad F_{\text{dt2}}^{(2)} = \tilde{F}_{\text{dt2}}^{(2)}(t) + \tilde{F}_{\text{dt2}}^{(2)}(u)\,, \tag{3.1}$$

where

$$\tilde{F}_{\text{dt1}}^{(2)}(t) = F_a^{(0)}(t)\left[F_a^{(1)}(t) + \frac{1}{2}\,F_a^{(0)}(t)\,\Pi_{gg}(t) - \frac{s\,(\epsilon\,(m_H^2 - 2p_T^2 + t) + 2p_T^2)}{(1-2\epsilon)(m_H^2 - s)t}\,F_d^{(1)}(t)\right], \tag{3.2}$$

and

$$\tilde{F}^{(2)}_{\rm dt2}(t) = F_a^{(0)}(t) \left[\frac{p_T^2}{t} \left(F_a^{(1)}(t) + \frac{1}{2}\, F_a^{(0)}(t)\, \Pi_{gg}(t) \right) - \frac{s\,(\epsilon\,(2p_T^2 - m_H^2 - t) + m_H^2 + t)}{(1-2\epsilon)(m_H^2 - s)t}\, F_d^{(1)}(t) \right] . \tag{3.3}$$

Here we have used eq. (2.5) and the fact that $F_d^{(0)}$ is zero. $\Pi_{gg}(q^2)$ is the transverse part of the one-loop gluon two-point function. Since the one-loop $gg^* \to H$ vertex is finite we need $\Pi_{gg}(q^2)$ only up to its finite part in ϵ. From eqs. (3.2) and (3.3) it is straightforward to obtain the corresponding formulae for the NLO (two-loop) corrections: in the square brackets one has to set Π_{gg} and $F_d^{(1)}$ to zero and replace $F_a^{(1)}$ by $F_a^{(0)}$.

Our result depends on the QCD gauge parameter which is introduced in the gluon propagator according to

$$D_g(q) = \frac{1}{i} \left(\frac{-g^{\mu\nu} + \xi \frac{q^\mu q^\nu}{-q^2}}{-q^2} \right) . \tag{3.4}$$

There are several available cross-checks for our calculation. First we find agreement with the exact two-loop result obtained in ref. [9]. Furthermore, we perform analytic and numerical comparisons in the large-m_t limit and cross check the results for the form factors $F_{\rm dt1}$ and $F_{\rm dt2}$ obtained in ref. [18], where an expansion up to order $1/m_t^8$ was performed. In this paper we have obtained expansions of the master integrals up to order $1/m_t^{100}$ in the expansion for $m_H \to 0$, using their differential equations.

In figure 6 we show the $\mathcal{O}(\epsilon^0)$ terms of the form factors $F^{(2)}_{\rm dt1}$ and $F^{(2)}_{\rm dt2}$ as a function of the partonic centre-of-mass energy $\sqrt{s}$, for several fixed values of the transverse momentum p_T between 50 GeV and 700 GeV. We note that in order to obtain physical quantities one has to combine the results presented in this paper with the one-particle irreducible contributions (which are a work-in-progress), perform the renormalization and add the contribution from additional real radiation. We have implemented our results in a flexible `Mathematica` code which can be used for such a combination, where the evaluation of the one-particle reducible form factors takes about one second per phase-space point. In the future we will also provide a high-performance `C++` implementation of both the one-particle reducible and irreducible NNLO form factors.

In the supplementary material of this paper we provide all results which are available analytically. This includes the m_H-expanded one-loop form factor $F_a^{(0)}$ including m_H^4 terms, and the small-q_s^2 expansion of the two-loop form factors $F_a^{(1)}$ and $F_d^{(1)}$ including $(q_s^2)^5$ terms.[3] The computer-readable code can be downloaded from ref. [60].

4 Conclusions

In this paper we provide an important ingredient which contributes to the NNLO virtual corrections for the process $gg \to HH$, namely the contribution from one-particle reducible

[3] We have computed the expansions up to order $(q_s^2)^{19}$; they can be obtained from the authors upon request.

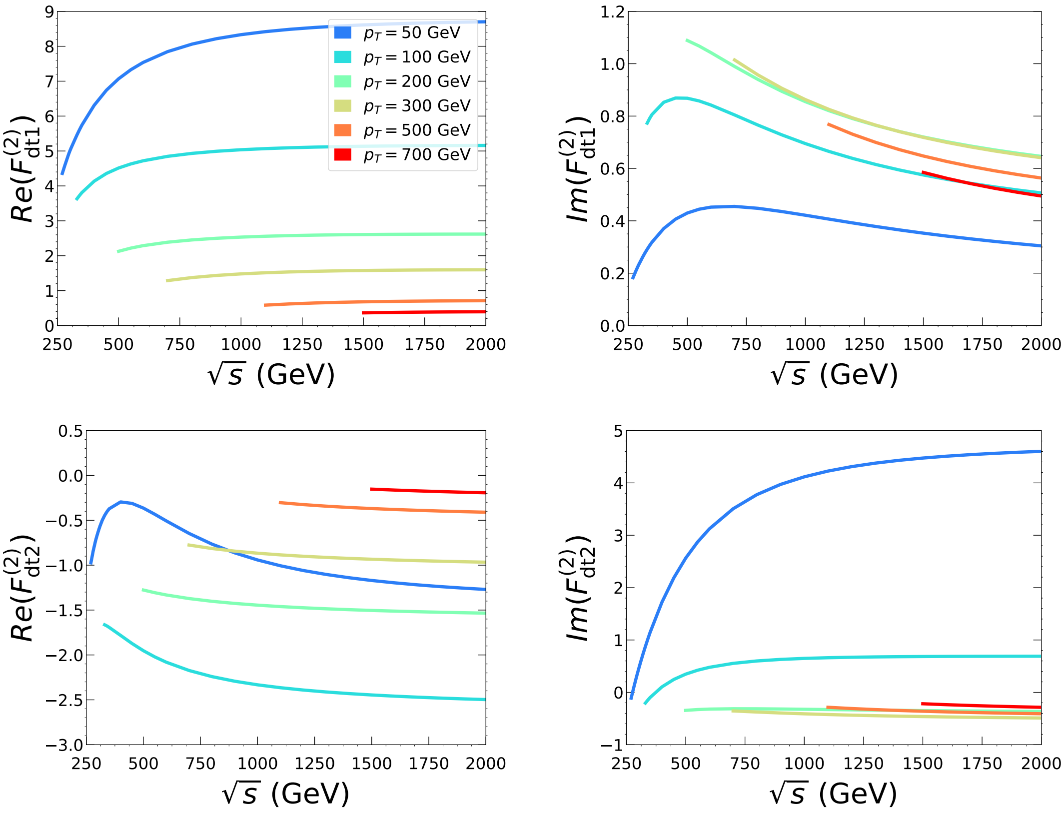

Figure 6. The finite parts of $F^{(2)}_{\mathrm{dt1}}$ and $F^{(2)}_{\mathrm{dt2}}$ as a function of $\sqrt{s}$, for various values of p_T. For the renormalization scale $\mu^2 = m_t^2$ has been chosen, and the gauge parameter $\xi = 0$.

diagrams. We describe in detail the calculation of the two-loop $gg^* \to H$ vertex with an off-shell gluon, which is used as building block. We obtain analytic results for the expansion around small gluon virtuality and "semi-analytic" results for the expansion for small m_H. The combination of both expansions provides a precise approximation of the off-shell $gg^* \to H$ vertex. Furthermore, we compute the one-loop corrections including terms of $\mathcal{O}(\epsilon^2)$. We present results for the bare form factors F_{dt1} and F_{dt2} which can easily be combined with other NNLO ingredients, once they are available.

Acknowledgments

This research was supported by the Deutsche Forschungsgemeinschaft (DFG, German Research Foundation) under grant 396021762 — TRR 257 "Particle Physics Phenomenology after the Higgs Discovery" and has received funding from the European Research Council (ERC) under the European Union's Horizon 2020 research and innovation programme grant agreement 101019620 (ERC Advanced Grant TOPUP). The work of JD is supported by the STFC Consolidated Grant ST/X000699/1.

References

[1] E.W.N. Glover and J.J. van der Bij, *Higgs boson pair production via gluon fusion*, *Nucl. Phys. B* **309** (1988) 282 [INSPIRE].

[2] T. Plehn, M. Spira and P.M. Zerwas, *Pair production of neutral Higgs particles in gluon-gluon collisions*, *Nucl. Phys. B* **479** (1996) 46 [hep-ph/9603205] [INSPIRE].

[3] S. Borowka et al., *Higgs Boson Pair Production in Gluon Fusion at Next-to-Leading Order with Full Top-Quark Mass Dependence*, *Phys. Rev. Lett.* **117** (2016) 012001 [*Erratum ibid.* **117** (2016) 079901] [arXiv:1604.06447] [INSPIRE].

[4] S. Borowka et al., *Full top quark mass dependence in Higgs boson pair production at NLO*, *JHEP* **10** (2016) 107 [arXiv:1608.04798] [INSPIRE].

[5] J. Baglio, F. Campanario, S. Glaus, M. Mühlleitner, M. Spira and J. Streicher, *Gluon fusion into Higgs pairs at NLO QCD and the top mass scheme*, *Eur. Phys. J. C* **79** (2019) 459 [arXiv:1811.05692] [INSPIRE].

[6] L. Bellafronte, G. Degrassi, P.P. Giardino, R. Gröber and M. Vitti, *Gluon fusion production at NLO: merging the transverse momentum and the high-energy expansions*, *JHEP* **07** (2022) 069 [arXiv:2202.12157] [INSPIRE].

[7] J. Davies, G. Mishima, K. Schönwald and M. Steinhauser, *Analytic approximations of* $2 \to 2$ *processes with massive internal particles*, *JHEP* **06** (2023) 063 [arXiv:2302.01356] [INSPIRE].

[8] J. Grigo, J. Hoff, K. Melnikov and M. Steinhauser, *On the Higgs boson pair production at the LHC*, *Nucl. Phys. B* **875** (2013) 1 [arXiv:1305.7340] [INSPIRE].

[9] G. Degrassi, P.P. Giardino and R. Gröber, *On the two-loop virtual QCD corrections to Higgs boson pair production in the Standard Model*, *Eur. Phys. J. C* **76** (2016) 411 [arXiv:1603.00385] [INSPIRE].

[10] J. Davies, G. Mishima, M. Steinhauser and D. Wellmann, *Double-Higgs boson production in the high-energy limit: planar master integrals*, *JHEP* **03** (2018) 048 [arXiv:1801.09696] [INSPIRE].

[11] J. Davies, G. Mishima, M. Steinhauser and D. Wellmann, *Double Higgs boson production at NLO in the high-energy limit: complete analytic results*, *JHEP* **01** (2019) 176 [arXiv:1811.05489] [INSPIRE].

[12] R. Bonciani, G. Degrassi, P.P. Giardino and R. Gröber, *Analytical Method for Next-to-Leading-Order QCD Corrections to Double-Higgs Production*, *Phys. Rev. Lett.* **121** (2018) 162003 [arXiv:1806.11564] [INSPIRE].

[13] R. Gröber, A. Maier and T. Rauh, *Reconstruction of top-quark mass effects in Higgs pair production and other gluon-fusion processes*, *JHEP* **03** (2018) 020 [arXiv:1709.07799] [INSPIRE].

[14] X. Xu and L.L. Yang, *Towards a new approximation for pair-production and associated-production of the Higgs boson*, *JHEP* **01** (2019) 211 [arXiv:1810.12002] [INSPIRE].

[15] G. Wang, Y. Wang, X. Xu, Y. Xu and L.L. Yang, *Efficient computation of two-loop amplitudes for Higgs boson pair production*, *Phys. Rev. D* **104** (2021) L051901 [arXiv:2010.15649] [INSPIRE].

[16] J. Baglio, F. Campanario, S. Glaus, M. Mühlleitner, J. Ronca and M. Spira, *$gg \to HH$: Combined uncertainties*, *Phys. Rev. D* **103** (2021) 056002 [arXiv:2008.11626] [INSPIRE].

JHEP08(2024)096

- [17] E. Bagnaschi, G. Degrassi and R. Gröber, *Higgs boson pair production at NLO in the POWHEG approach and the top quark mass uncertainties*, *Eur. Phys. J. C* **83** (2023) 1054 [arXiv:2309.10525] [INSPIRE].
- [18] J. Davies and M. Steinhauser, *Three-loop form factors for Higgs boson pair production in the large top mass limit*, *JHEP* **10** (2019) 166 [arXiv:1909.01361] [INSPIRE].
- [19] J. Davies, F. Herren, G. Mishima and M. Steinhauser, *Real corrections to Higgs boson pair production at NNLO in the large top quark mass limit*, *JHEP* **01** (2022) 049 [arXiv:2110.03697] [INSPIRE].
- [20] J. Grigo, J. Hoff and M. Steinhauser, *Higgs boson pair production: top quark mass effects at NLO and NNLO*, *Nucl. Phys. B* **900** (2015) 412 [arXiv:1508.00909] [INSPIRE].
- [21] J. Davies, K. Schönwald and M. Steinhauser, *Towards $gg \to HH$ at next-to-next-to-leading order: Light-fermionic three-loop corrections*, *Phys. Lett. B* **845** (2023) 138146 [arXiv:2307.04796] [INSPIRE].
- [22] S. Catani, *The Singular behavior of QCD amplitudes at two loop order*, *Phys. Lett. B* **427** (1998) 161 [hep-ph/9802439] [INSPIRE].
- [23] P. Nogueira, *Automatic Feynman Graph Generation*, *J. Comput. Phys.* **105** (1993) 279 [INSPIRE].
- [24] M. Gerlach, F. Herren and M. Lang, *tapir: A tool for topologies, amplitudes, partial fraction decomposition and input for reductions*, *Comput. Phys. Commun.* **282** (2023) 108544 [arXiv:2201.05618] [INSPIRE].
- [25] R. Harlander, T. Seidensticker and M. Steinhauser, *Complete corrections of $O(\alpha\alpha_s)$ to the decay of the Z boson into bottom quarks*, *Phys. Lett. B* **426** (1998) 125 [hep-ph/9712228] [INSPIRE].
- [26] T. Seidensticker, *Automatic application of successive asymptotic expansions of Feynman diagrams*, in the proceedings of the *6th International Workshop on New Computing Techniques in Physics Research: Software Engineering, Artificial Intelligence Neural Nets, Genetic Algorithms, Symbolic Algebra, Automatic Calculation*, Heraklion, Greece, 12–16 April 1999, hep-ph/9905298 [INSPIRE].
- [27] B. Ruijl, T. Ueda and J. Vermaseren, *FORM version 4.2*, arXiv:1707.06453 [INSPIRE].
- [28] J. Klappert, F. Lange, P. Maierhöfer and J. Usovitsch, *Integral reduction with Kira 2.0 and finite field methods*, *Comput. Phys. Commun.* **266** (2021) 108024 [arXiv:2008.06494] [INSPIRE].
- [29] R.N. Lee, *LiteRed 1.4: a powerful tool for reduction of multiloop integrals*, *J. Phys. Conf. Ser.* **523** (2014) 012059 [arXiv:1310.1145] [INSPIRE].
- [30] E. Remiddi and J.A.M. Vermaseren, *Harmonic polylogarithms*, *Int. J. Mod. Phys. A* **15** (2000) 725 [hep-ph/9905237] [INSPIRE].
- [31] A. von Manteuffel and L. Tancredi, *A non-planar two-loop three-point function beyond multiple polylogarithms*, *JHEP* **06** (2017) 127 [arXiv:1701.05905] [INSPIRE].
- [32] M. Fael, F. Lange, K. Schönwald and M. Steinhauser, *A semi-analytic method to compute Feynman integrals applied to four-loop corrections to the $\overline{MS}$-pole quark mass relation*, *JHEP* **09** (2021) 152 [arXiv:2106.05296] [INSPIRE].
- [33] M. Fael, F. Lange, K. Schönwald and M. Steinhauser, *Massive Vector Form Factors to Three Loops*, *Phys. Rev. Lett.* **128** (2022) 172003 [arXiv:2202.05276] [INSPIRE].
- [34] M. Fael, F. Lange, K. Schönwald and M. Steinhauser, *Singlet and nonsinglet three-loop massive form factors*, *Phys. Rev. D* **106** (2022) 034029 [arXiv:2207.00027] [INSPIRE].

JHEP08(2024)096

[35] M. Fael, F. Lange, K. Schönwald and M. Steinhauser, *Massive three-loop form factors: Anomaly contribution*, *Phys. Rev. D* **107** (2023) 094017 [arXiv:2302.00693] [INSPIRE].

[36] M. Spira, A. Djouadi, D. Graudenz and P.M. Zerwas, *Higgs boson production at the LHC*, *Nucl. Phys. B* **453** (1995) 17 [hep-ph/9504378] [INSPIRE].

[37] R. Harlander and P. Kant, *Higgs production and decay: Analytic results at next-to-leading order QCD*, *JHEP* **12** (2005) 015 [hep-ph/0509189] [INSPIRE].

[38] C. Anastasiou, S. Beerli, S. Bucherer, A. Daleo and Z. Kunszt, *Two-loop amplitudes and master integrals for the production of a Higgs boson via a massive quark and a scalar-quark loop*, *JHEP* **01** (2007) 082 [hep-ph/0611236] [INSPIRE].

[39] U. Aglietti, R. Bonciani, G. Degrassi and A. Vicini, *Analytic Results for Virtual QCD Corrections to Higgs Production and Decay*, *JHEP* **01** (2007) 021 [hep-ph/0611266] [INSPIRE].

[40] R.V. Harlander and K.J. Ozeren, *Top mass effects in Higgs production at next-to-next-to-leading order QCD: Virtual corrections*, *Phys. Lett. B* **679** (2009) 467 [arXiv:0907.2997] [INSPIRE].

[41] J. Ablinger, J. Blümlein, P. Marquard, N. Rana and C. Schneider, *Automated Solution of First Order Factorizable Systems of Differential Equations in One Variable*, *Nucl. Phys. B* **939** (2019) 253 [arXiv:1810.12261] [INSPIRE].

[42] J. Blümlein and S. Kurth, *Harmonic sums and Mellin transforms up to two loop order*, *Phys. Rev. D* **60** (1999) 014018 [hep-ph/9810241] [INSPIRE].

[43] J.A.M. Vermaseren, *Harmonic sums, Mellin transforms and integrals*, *Int. J. Mod. Phys. A* **14** (1999) 2037 [hep-ph/9806280] [INSPIRE].

[44] J. Blümlein, *Structural Relations of Harmonic Sums and Mellin Transforms up to Weight $w = 5$*, *Comput. Phys. Commun.* **180** (2009) 2218 [arXiv:0901.3106] [INSPIRE].

[45] J. Ablinger, *A Computer Algebra Toolbox for Harmonic Sums Related to Particle Physics*, MSc Thesis, Johannes Kepler Universität Linz, Linz, Austria (2009) [arXiv:1011.1176] [INSPIRE].

[46] J. Ablinger, J. Blümlein and C. Schneider, *Harmonic Sums and Polylogarithms Generated by Cyclotomic Polynomials*, *J. Math. Phys.* **52** (2011) 102301 [arXiv:1105.6063] [INSPIRE].

[47] J. Ablinger, *Computer Algebra Algorithms for Special Functions in Particle Physics*, Ph.D. Thesis, Johannes Kepler Universität Linz, Linz, Austria (2012) [arXiv:1305.0687] [INSPIRE].

[48] J. Ablinger, J. Blümlein and C. Schneider, *Generalized Harmonic, Cyclotomic, and Binomial Sums, their Polylogarithms and Special Numbers*, *J. Phys. Conf. Ser.* **523** (2014) 012060 [arXiv:1310.5645] [INSPIRE].

[49] J. Ablinger, J. Blümlein and C. Schneider, *Analytic and Algorithmic Aspects of Generalized Harmonic Sums and Polylogarithms*, *J. Math. Phys.* **54** (2013) 082301 [arXiv:1302.0378] [INSPIRE].

[50] J. Ablinger, J. Blümlein, C.G. Raab and C. Schneider, *Iterated Binomial Sums and their Associated Iterated Integrals*, *J. Math. Phys.* **55** (2014) 112301 [arXiv:1407.1822] [INSPIRE].

[51] J. Ablinger, *The package HarmonicSums: Computer Algebra and Analytic aspects of Nested Sums*, *PoS* **LL2014** (2014) 019 [arXiv:1407.6180] [INSPIRE].

[52] J. Ablinger, *Discovering and Proving Infinite Binomial Sums Identities*, *Exp. Math.* **26** (2016) 62 [arXiv:1507.01703] [INSPIRE].

[53] J. Ablinger, *Computing the Inverse Mellin Transform of Holonomic Sequences using Kovacic's Algorithm*, *PoS* **RADCOR2017** (2018) 001 [arXiv:1801.01039] [INSPIRE].

[54] C. Schneider, *Symbolic summation assists combinatorics*, *Sémin. Lothar. Comb.* **56** (2007) 1.

[55] C. Schneider, *Term Algebras, Canonical Representations and Difference Ring Theory for Symbolic Summation*, arXiv:2102.01471.

[56] B. Jantzen, A.V. Smirnov and V.A. Smirnov, *Expansion by regions: revealing potential and Glauber regions automatically*, *Eur. Phys. J. C* **72** (2012) 2139 [arXiv:1206.0546] [INSPIRE].

[57] C. Schneider, *Simplifying Multiple Sums in Difference Fields*, in *Computer Algebra in Quantum Field Theory: Integration, Summation and Special Functions*, C. Schneider and J. Bluemlein eds., *Texts and Monographs in Symbolic Computation*, Springer (2013), pp. 325–360 [DOI:10.1007/978-3-7091-1616-6_14] [arXiv:1304.4134] [INSPIRE].

[58] J. Ablinger, J. Blümlein, P. Marquard, N. Rana and C. Schneider, *Three loop QCD corrections to heavy quark form factors*, in the proceedings of the *19th International Workshop on Advanced Computing and Analysis Techniques in Physics Research: Empowering the revolution: Bringing Machine Learning to High Performance Computing (ACAT 2019)*, Saas-Fee, Switzerland, 11–15 March 2019, *J. Phys. Conf. Ser.* **1525** (2020) 012018 [arXiv:1905.03728] [INSPIRE].

[59] X. Liu and Y.-Q. Ma, *AMFlow: A Mathematica package for Feynman integrals computation via auxiliary mass flow*, *Comput. Phys. Commun.* **283** (2023) 108565 [arXiv:2201.11669] [INSPIRE].

[60] J. Davies, K. Schoenwald, M. Steinhauser and M. Vitti. *TTP24-016 Three-loop corrections to Higgs boson pair production: reducible contribution*, https://www.ttp.kit.edu/preprints/2024/ttp24-016/.

JHEP08(2024)096